Tohoku J. Exp. Med., 2000, **190**, 65-82

Review

Pathogenesis of Nonimmune Hydrops Fetalis Caused by Intrauterine B19 Infection

NOBUO YAEGASHI

Department of Obstetrics and Gynecology, Tohoku University School of Medicine, Sendai 980-8574

YAEGASHI, N. *Pathogenesis of Nonimmune Hydrops Fetalis Caused by Intrauterine B19 Infection.* Tohoku J. Exp. Med., 2000, **190** (2), 65-82 —— Intrauterine human parvovirus B19 infection is related to non-immune hydrops fetalis and fetal death. First, we performed epidemiological studies to determine the critical period during which maternal infection led to hydrops fetalis. The studies showed that the hepatic period of hematopoietic activity was correlated with the critical period of maternal infection, which suggested that B19 might have affinity for erythroid lineage cells at the stage of hematopoiesis. We next established an in vitro infection experimental system of B19 using erythroid lineage cells derived from fetal liver cells. We demonstrated that the erythroid lineage cells proved to be appropriate targets for B19 virus and that B19 infection could induce apoptosis of infected cells. The massive destruction of erythroid lineage cells through apoptosis seems to cause severe anemia and to result in heart failure of the fetus. To analyze the cytotoxic mechanism in more detail, we established a stringent regulatory expression system of the NS1 protein encoded by the B19 genome and indicated that the apoptosis induced by B19 was directly caused by the NS1 protein. Experiments using mutations engineered in the ATP-binding domain of NS1 indicated that this domain played a critical role for the apoptosis induction. The present studies may contribute to a better understanding of the pathogenesis of hydrops fetalis associated with B19 infection during pregnancy. ———— parvovirus B19; pregnancy; hydrops fetalis; apoptosis; NS1

Human parvovirus B19 was first discovered in the plasma of a healthy individuals by Cossart et al. (1975). The virions are non-enveloped, 15- to 28 nm-diameter particles with icosahedral symmetry (Fig. 1). The B19 genome consists of a single strand DNA of approximately 5500 nucleotides (Fig. 2). The three major viral proteins, one non-structural protein and two capsid proteins (VP1, 84kDa; VP1, 58kDa) were encoded in the genome. The only nonstructural

Received January 27, 2000; revision accepted for publication February 10, 2000.

Address for reprints: Nobuo Yaegashi, Department of Obstetrics and Gynecology, Tohoku University School of Medicine, Sendai 980-8574, Japan.

e-mail: nyaegashi@gonryo.med.tohoku.ac.jp

Dr. N. Yaegashi is a recipient of the 1999 Gold Prize, Tohoku University School of Medicine.

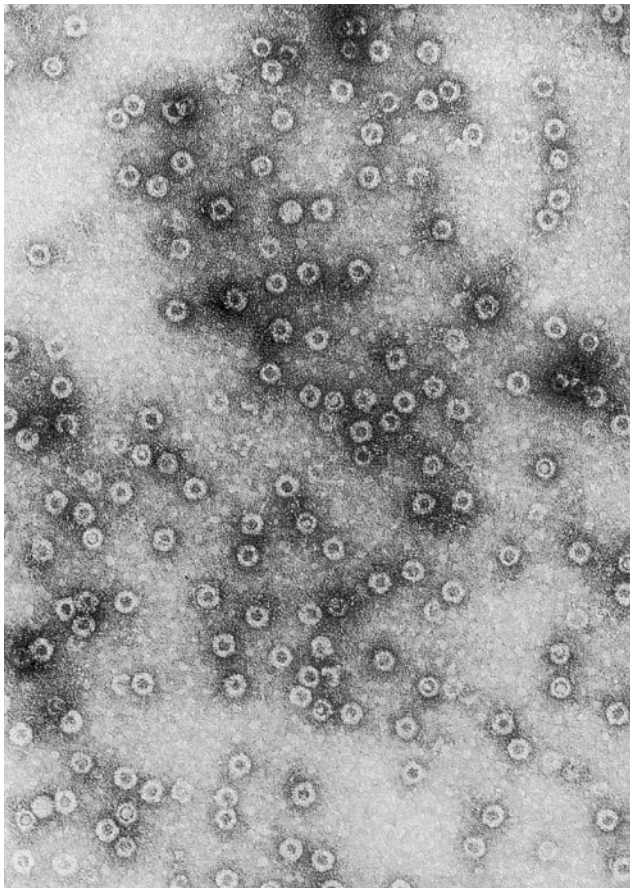

Fig. 1. Electron microscopic appearence of the B19 viral particles.

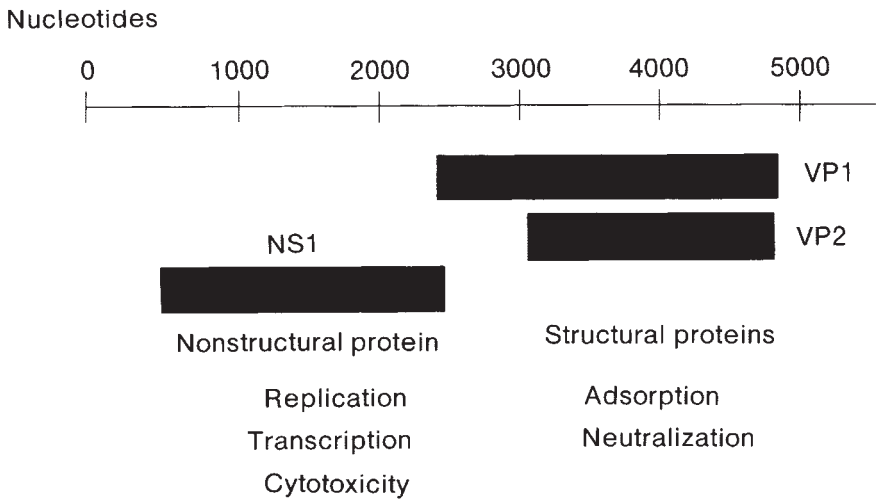

Fig. 2. Genomic structure and encoded proteins of parvovirus B19.

protein (NS1, 77kDa) is a phosphoprotein. Consistent with its role in viral propagation, the protein has DNA-binding properties, adenosine and guanosine triphosphate activity, and nuclear localization signals (Brown and Young 1998).

B19 virus is now known to be etiologically related to human illnesses including erythema infectiosum (fifth disease) (Shiraishi et al. 1985), thrombocytopenia and purpura (Shiraishi et al. 1989), arthritis (Shiraishi et al. 1991), meningitis and neurologic disease, myocarditis, hepatitis, vasculitis, rheumatic arthritis (Sasaki et

al. 1989, 1995), transient aplastic crisis, chronic bone marrow failure, and so on.

Only erythroid progenitor cells derived from bone marrow had been demonstrated to be a target cell population for in vitro B19 virus infection at a point of time when we started the present study in 1987. When B19 virus was inoculated into a culture of bone marrow cells, erythroid colony formation was significantly inhibited. This suggests that the aplastic crisis could result from infection of erythroid progenitor cells with B19 virus. However, pathogenesis of other diseases associated with B19 virus infection was still unknown.

In 1984, the first association between intrauterine B19 infection and nonimmune hydrops fetalis (NIHF) and stillbirth (Brown et al. 1984; Knott et al. 1984). Subsequently, several retrospective and prospective studies had been published that provide a risk assessment of fetal loss after a maternal infection. However, these studies were a long way from providing a real understanding of the pathogenesis of hydrops fetalis. There had been few studies of B19 infection in Japan. Hydrops fetalis is thought to be caused by infection of fetal erythroid progenitor cells with B19 infection during pregnancy. B19 infection has been speculated to cause the destruction of erythroid progenitor cells, generating the development of severe anemia and heart failure. Consequently, the fetus falls into a hydropic state, resulting in intrauterine fetal death. Actually, a typical characteristic of NIHF caused by intrauterine B19 infection is severe anemia of the fetus (Fig. 2).

Under these circumstances in 1987, we started a project to clarify the pathogenesis of fetal death and hydrops fetalis caused by intrauterine B19 infection. This project has been a joint collaboration of the Department of Obstetrics and Gynecology (Professor Akira Yajima and Professor Kunihiro Okamura) and the Department of Microbiology and Immunology (Professor Kazuo Sugamura).

Intrauterine B19 infection as a cause of NIHF

We analyzed over 100 reports describing the relationship between B19 infection and pregnancy, the fetus and/or the newborn (Yaegashi et al. 1994, 1995, 1998). Studies were identified by a computer search of Index Medicus and from the reference of each report. Duplicated cases were avoided by referring to the clinical history and/or pathological findings when more than one relevant paper originated from the same institution. To calculate the incidence of B19 infection among etiologically-unknown cases of NIHF with minimizing biases, we selected 11 literatures which studied more than 10 cases of NIHF. In the 11 studies selected, 1194 cases of NIHF were enrolled. Chromosome abnormalities, twin-to-twin transfusion syndrome (TTTS), and many kinds of malformations including cardiovascular anomalies, were identified as the major causes of NIHF. After excluding these factors, the remaining 299 cases, including our cases, were etiologically-unknown and/or anatomically-normal cases. Intrauterine B19 infection was diagnosed by the presence of B19 DNA in fetal tissues or the

placenta or by the histological confirmation of characteristic nuclear inclusions in erythroid cells. B19 infection was found to be responsible for 57 of the 299 cases, i.e., the incidence of parvovirus infection among etiologically-unknown cases of NIHF was 19.1% (14.5%-23.7%: 95% confidence interval).

Risk of adverse fetal outcome among women infected during pregnancy

To calculate the risk of adverse outcome among women who had acquired parvovirus B19 infection antenatally, we identified 24 prospective studies which followed pregnant women positive for IgM specific to parvovirus B19 by screening tests, or pregnant women who had a chance to contact B19 infectious sources and/or had maternal symptoms related to B19 infection (Yaegashi et al. 1998). We analyzed 620 women with antenatal B19 infection in the published data, including ours (Yaegashi et al. 1999a). Pregnant women were tested for B19 IgM and IgG positivity. Acute B19 infection was diagnosed in women who were IgM-positive or who had seroconversion for B19 antibodies in serum; these women were followed-up until delivery. NIHF was the typical adverse outcome, although pregnancies resulting in spontaneous abortions and still births without manifestation of NIHF were also included in some studies. Fetal tissues, cord blood, and the placentae were analyzed for the presence of B19 DNA by PCR or DNA hybridization techniques. The adverse outcome was definitively attributed to intrauterine B19 infection only in cases positive for B19 DNA.

Of the 620 pregnant women, 96 fetuses (15.5%) had adverse outcomes. The adverse outcome was definitively attributed to B19 infection, as confirmed by detection of B19 DNA in fetal tissue or the placenta in 57 (10.2%) of 557 fetuses. Thus, the excess risk of fetal death due to B19 in women infected during pregnancy, excluding cases in which tissues were not examined for B19 DNA, was 10.2%. When we limited the analysis to women who became infected during the first 20 weeks of pregnancy, the excess risk of an adverse risk associated with an intrauterine B19 infection was estimated at 12.4% (30/242).

Fetal death did not result in any of the definitive cases although only a few of the mothers in these cases became infected later than 20 weeks.

Rates of vertical (transplacental) transmission

Vertical transmission was identified by the presence of at least one of the following features: An adverse outcome with virological findings in fetal tissues or products of conception, B19 IgM positivity in cord or neonatal blood, persistent B19 IgG in infants aged over one year, or prenatal confirmation of fetal infection. Transplacental transmission was confirmed in 69 (24.1%) of 286 cases. Among the infected babies who survived, there were neither congenital anomalies nor serious neuro-developmental problems.

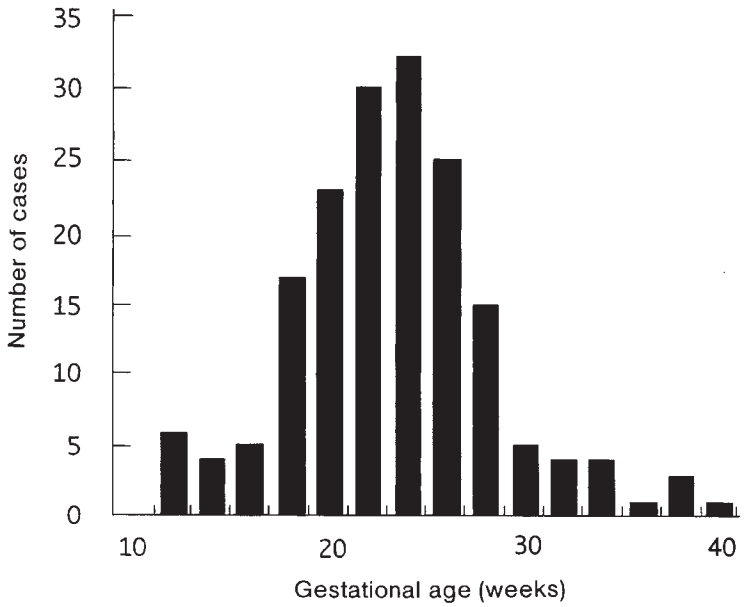

Fig. 3. Gestational weeks of diagnosis of NIHF in 165 cases from 80 literatures.

Gestational week at diagnosis of NIHF

The clinical details were available for 165 cases, derived from 80 literatures. The gestational age at the time of diagnosis of NIHF ranged from 11 to 39 weeks, with the peak occurring at 23 to 24 weeks (Fig. 3). NIHF was diagnosed in the second trimester (17 to 28 weeks) in 135 cases (82%). The mean gestational age at the time of diagnosis was 22.8 ± 5.1 weeks.

Interval between the onset of maternal infection and diagnosis of NIHF

To calculate the mean gestational age at the time of diagnosis of NIHF caused by B19 infection, and interval between the onset of maternal infection and diagnosis of NIHF, we analyzed 165 cases from 80 literatures , for which the clinical details were available.

The presence or absence of maternal symptoms of infection were described for 98 (59%) of 165 cases. Maternal symptoms of infection were present in 62 (63%) of 98 cases (63%). The interval between the onset of symptoms and the diagnosis of NIHF was described in 49 (79%) of 62 cases. Data on the gestational week of the mother's exposure to the source of infection was available for only 6 of 36 asymptomatic mothers. In those 6 women, the onset of maternal symptoms was estimated to occur 1 week after exposure to the source of infection. Thus, we analyzed data for 55 cases. The interval between the onset of maternal B19 infection and diagnosis of NIHF ranged from 1 to 17 weeks; 2 weeks or less in 8 cases, 3-4 weeks in 13 cases, 5-6 weeks in 13 cases, 7-8 weeks in 7 cases, 9-10 weeks in 6 cases, 11-12 weeks in 5 cases, and 13-17 weeks in 3 cases (Fig. 4). Although NIHF was diagnosed up to 17 weeks after the onset of maternal illness, 47 (85%) of 55 cases were diagnosed within 10 weeks (mean: 6.2 ± 3.7 weeks).

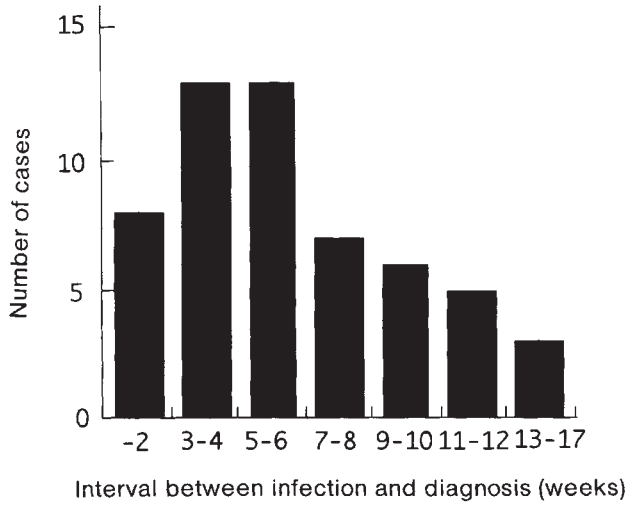

Fig. 4. Interval between the onset of maternal infection and diagnosis of NIHF or fetal death.

Estimation of the critical period during which maternal infection led to NIHF

We attempted to gain an estimate of the incidence of NIHF according to onset of maternal infection, and therefore an indication of the critical period during which maternal infection will frequently lead to NIHF or fetal death. We analyzed 67 cases with antenatal B19 infection resulting in NIHF in the published data, including our own. The gestational age at the onset of maternal infection ranged from 6 weeks to 39 weeks of gestation, with the peak occurring between 13-

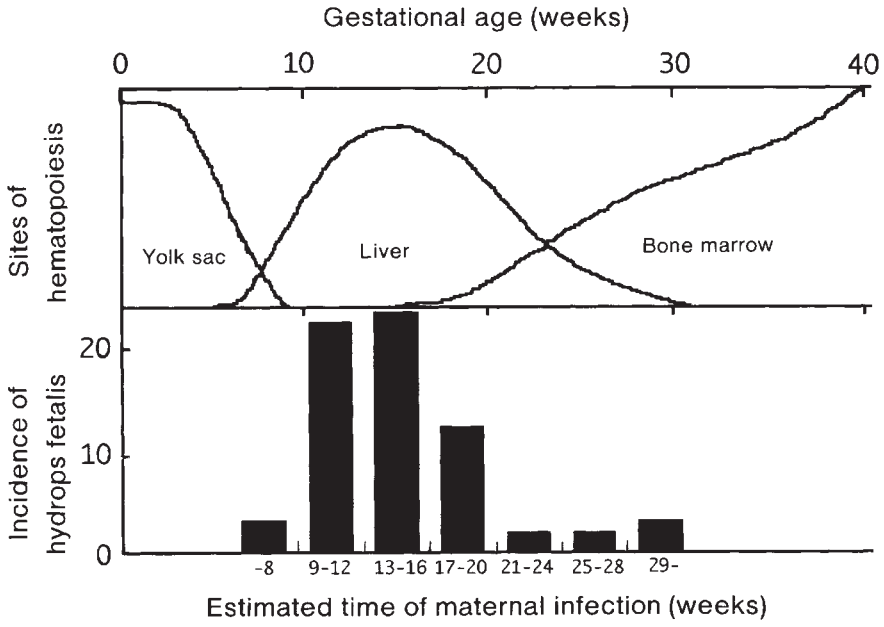

Fig. 5. Estimation of the critical period during which maternal infection leads to NIHF. Upper panel: Sites and activity of hematopoiesis in the human fetus by gestational week. Lower panel: The incidence of NIHF acccording to the gestational week when the maternal infection was expected to have occurred. The peak correlated with the hepatic period of hematopoietic activity.

16 weeks (Fig. 5). The sites and activity of fetal hematopoiesis by gestational week were also shown in the same figure. The incidence of NIHF by gestational week correlated with the hepatic period of hematopoieic activity.

Outbreaks of erythema infectiosum and hydrops fetalis caused by B19 infection

Between July 1987 and June 1997, there were approximately 25 000 births per year in Miyagi prefecture. During that period, 168 cases of NIHF were diagnosed at the Tohoku University Hospital by ultrasound with the formation and accumulation of serous fluid in body cavities and subcutaneous edema. Ultrasonography, fetal karyotyping, fetal echocardiography, pathological studies for placentae and cords, serological tests for TORCH (toxoplasma, rubella, cytomegalovirus, herpes) syndrome were performed to identify an etiology of hydrops fetalis. Cases of hydrops fetalis with heart anomalies, congenital malformations, multiple pregnancy, abnormal karyotypes, cystic hygroma, or chorioangioma of the placenta were excluded. No cases had immunologic causes, i.e., isoimmunization due to Rhesus blood group incompatibility, ABO blood group incompatibility, or other blood group incompatibilities. Of the 168 cases of NIHF, 66 cases were diagnosed as etiology-unknown. Maternal serum, cord blood and placental specimens from cases of NIHF were collected and stored at $-80^{\circ}C$ until analyzing for B19 IgM and IgG antibodies by ELISA, and for B19 DNA by PCR with informed consent. B19 infection was diagnosed based on the presence of B19 IgM in serum or the presence of B19 DNA.

In total, 13 of 168 cases of hydrops fetalis were found to have been caused by B19 intrauterine infection in Miyagi prefecture during the study period. B19 infection was diagnosed when the serum or the placental tissue was positive for B19 IgM or B19 DNA. Hydrops fetalis was diagnosed prenatally with ultrasonography in all 13 cases. In 12 of the 13 cases, the fetus had already died in utero by the time of diagnosis. In the remaining case, the fetus was alive when hydrops fetalis was diagnosed at 22 gestational weeks. The fetus had severe anemia (hemoglobin, 4.6 g/100 ml; hematocrit, 9.6%), and was treated with three intrauterine transfusions, survived, and was delivered normally at term.

Since 1981, we have monitored the number of cases of erythema infectiosum in Miyagi prefecture each month through a network of 70 pediatric clinics. According to the monthly number of cases of erythema infectiosum, two outbreaks of erythema infectiosum occurred in the 10 years surveyed: from the spring of 1990 through the summer of 1992 and from the spring of 1996 through the spring of 1997. We found that 12 of the 13 cases of hydrops fetalis clustered during outbreaks of erythema infectiosum: 5 during the first outbreak and 7 during the second outbreak (Fig. 6). In contrast, the incidence of the remaining 155 cases of hydrops fetalis, unrelated to B19, had been almost constant during the 10 years and was not correlated with outbreaks of erythema infectiosum. The percentage of hydrops fetalis caused by B19 during epidemic periods (12%, 12/99) was

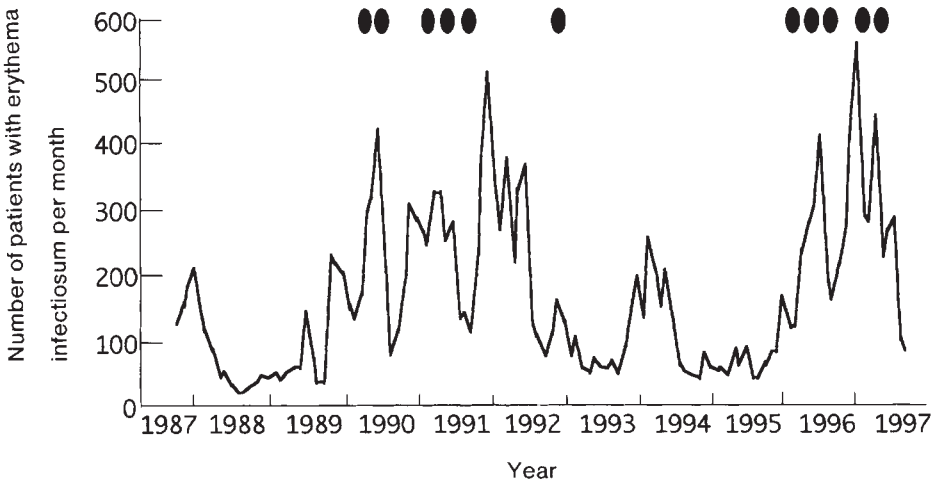

Fig. 6. Cases of hydrops fetalis caused by intrauterine parvovirus B19 infection and the monthly reported number of cases of erythema infectiosum in Miyagi Prefecture (1987-1997). One closed oval is one case of hydrops fetalis caused by B19.

significantly higher than that (1%, 1/69) during non-epidemic periods ($p<0.05$, chi-square test). In epidemic periods, 44% (12/27) of hydrops cases in which the etiology was unknown were caused by B19 intrauterine infection and 5% (1/21) during non-epidemic periods (Yaegashi et al. 1995, 1999a).

Change of the positive rates of B19 antibodies among pregnant women during the past 10 years

To investigate changes in the positive rate of B19 antibodies in pregnant women during the past 10 years, sera were obtained from 232 pregnant women in 1987 and 277 in 1997, who visited our obstetric clinics for diagnosis of pregnancy. Blood was drawn for blood typing and syphilis test and hepatitis B tests, which are routine tests for pregnant women in Japan, at their 6th to 12th weeks of gestation. This blood was stored at -80°C until assayed and used for B19 test with informed consent.

In total, sera from 509 pregnant women were tested for B19 IgG and IgM and overall IgG positive rate was 40% (203/509) and IgM, 1.8% (9/509) (Table 1).

The overall positive rate of B19 IgG antibody was significantly higher in 1997 (46%, 126/277) than in 1987 (33%, 77/232). However, age-specific positive rates differed significantly between 1987 and 1997 only in women aged 20 to 24 years and in those aged 25 to 29 years ($p<$ 0.05, chi-square test) (Yaegashi et al. 1990, 1999a).

Sera from 3 of 232 women (1.3%) in 1987, and 6 of 277 women (2.2%) in 1997 were positive for B19 IgM. There was no statistical difference between the two groups. All 9 women whose sera were positive for IgM gave birth to healthy babies.

TABLE 1. *Comparison of the age-specific B19 IgG prevalence between 1987 and 1997*

Age (Year)	1987	1997	
20-24	33% (11/33)	58% (23/40)	$p<0.05$[a]
25-29	20% (21/107)	48% (59/122)	$p<0.05$
30-34	43% (29/68)	31% (26/85)	N.S.[b]
35-39	67% (16/24)	60% (18/30)	N.S.
Total	33% (77/232)	46% (126/277)	$p<0.05$

[a]Chi-square test.
[b]No significant difference.

Establishment of monoclonal antibodies against parvovirus B19 capsid antigens

Monoclonal antibodies against parvovirus are required to establish the diagnostic procedure for B19 infection. B19 virions were purified from the plasma of a blood donor who was found to have B19 viremia. A BALB/c mouse was immunized with 50 μg of the purified B19 virions mixed with complete Freund adjuvant. The spleen was removed and the spleen cells were fused with SP2/0-Agl4 myeloma cells. The hybridoma cells were screened for production of anti-B19 monoclonal antibodies by an enzyme-linked immunosorbent assay (ELISA).

Fifteen hybridoma clones isolated independently produced antibodies positive for the B19-specific ELISA. The specificity was further examined by the

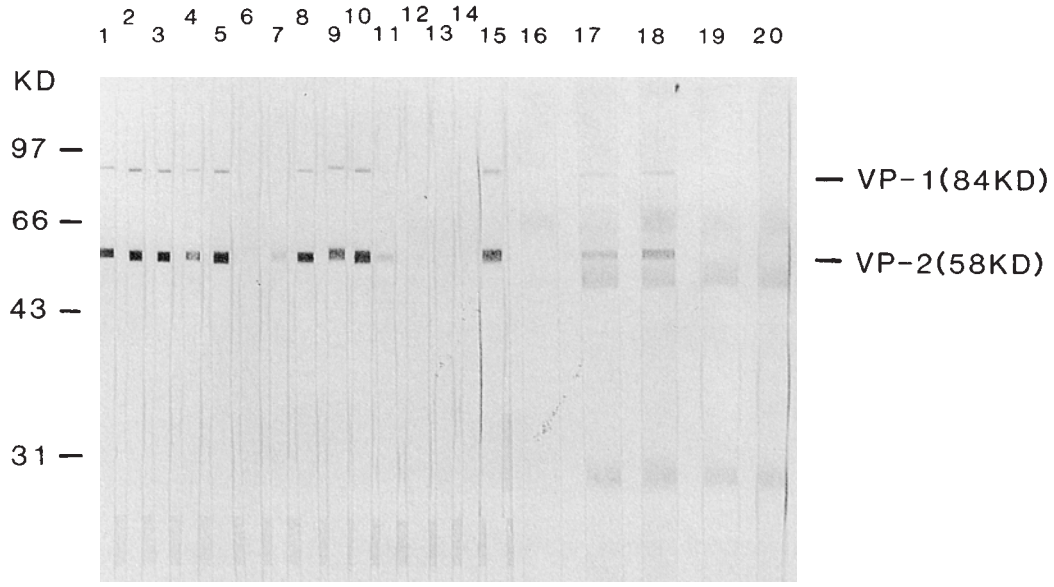

Fig. 7. Monoclonal antibodies against the capsid proteins of B19 virion. The Western blotted B19 antigen was detected with monoclonal antibodies of 15 clones (Lanes 1 to 15) positive in ELISA screening, with H-31 monoclonal antibody against interleukin 7 receptor α chain (Lane 16, negative control), and with anti-B19 positive (Lanes 17 and 18) and negative (Lanes 19 and 20) human sera.

Western blot immunoassay (Fig. 7). Monoclonal antibodies produced by eleven of these clones detected both 84 and 58 kDa peptides of B19 virions. These clones were named PAR1-5, PAR7-11, and PAR15, respectively. Anti-B19 positive human sera also detected the 84 and 58 kDa peptides but not negative sera. The specificity of the monoclonal antibodies was also examined by indirect double immunofluorescence staining with B19-infected fetal erythroid cells. These monoclonal antibodies immunoprecipitated B19 virions (Yaegashi et al. 1989a, b).

Detection of B19-infected cells in fetal tissues

We examined tissues from nine fetuses who had died of hydrops fetalis caused by intrauterine B19 infection. Hydrops fetalis was diagnosed at 18 to 31 weeks of gestation with ultrasonography. An autopsy diagnosis of hydrops fetalis or the

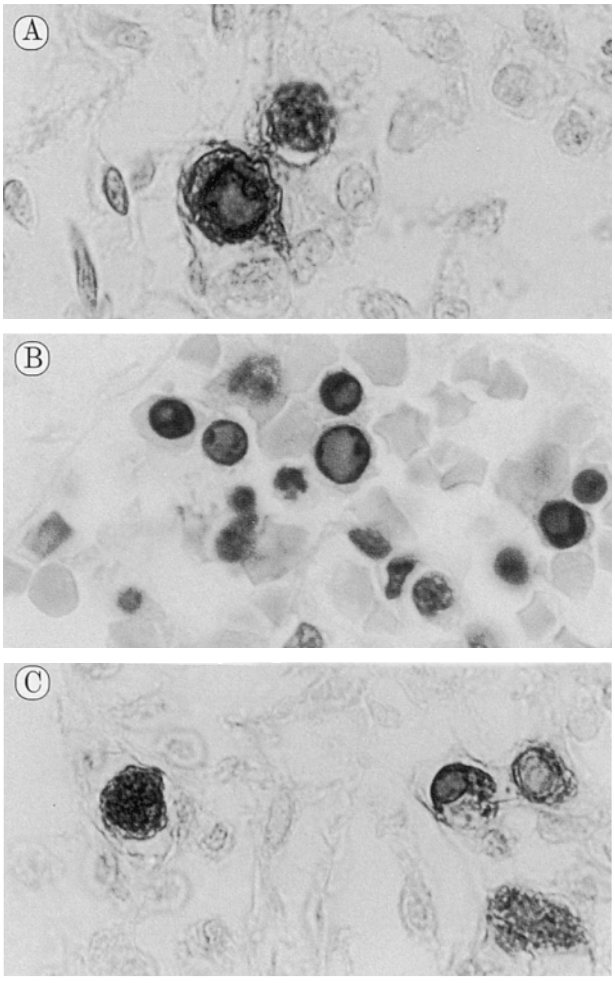

Fig. 8. (A) Immunohistochemical staining of fetal lung tissues with PAR3. Only erythroid cells in cases of hysrops fetalis caused bt B19 were positive for PAR3. (B) Light microscopic findings of B19-infected cells in fetal tissues. Fetal kidney tissues were stained with H & E. Erythroid cells of fetal tissues in cases of B19 infection showed characteristic nuclear inclusions. (C) TUNEL immunostaining of fetal tissues. Tissues from cases of hydrops fetalis caused by B19 infection were stained with the TUNEL method using peroxidase and diaminobenzidine.

mention of large amount of ascitic, pleural or subcutaneous fluid in the autopsy report was critical for these cases to be included in this study. B19 DNA in fetal tissues was demonstrated with the polymerase chain reaction in all cases. Tissues obtained at autopsy in four cases of hydrops fetalis caused by heart anomaly, chromosomal abnormalities, or twin-to-twin transfusion syndrome were used as negative controls. Tissues available in most cases included the lungs, kidneys, liver, spleen, and heart. This study was approved by the Ethic Committee of Tohoku University School of Medicine.

Tissues were immunohistochemically stained with PAR3 (anti-B19 monoclonal antibody). In tissues from each of the nine cases, erythrocyte precursors were intensely stained with PAR3 (Fig. 8A), confirming the presence of B19 viral proteins in these cells (Yaegashi et al. 1999b). The percentage of erythroid cells that were positive for PAR3 ranged from 10.3% to 32.4% and was higher in liver tissue than in other tissues ($p<0.05$, chi-square test). The percentage of PAR3-positive cells correlated well with that of cells with nuclear inclusions. Tissues or cells other than erythroid cells were not positive for PAR3. Heart tissue was available in five cases, but no cardiac myocytes were positive for PAR3. No positive signals were detected in control tissues.

Apoptosis of infected cells in fetal tissues

The prevalence of intranuclear inclusions characteristic of parvovirus B19 infection were assessed in each of the cases. Inclusions in erythrocyte precursors were noted in all cases (Fig. 8B). All cases of parvovirus infection had histologically diagnostic inclusions in multiple tissues, but parvovirus inclusions were not seen in any cell types other than erythroid cells. Inclusions were seen in 13.8% to 36.6% of erythroid cells, and the prevalence of inclusions in each case was higher in the liver than in other tissues ($p<0.05$, chi-square test). Cells containing nuclear inclusions often had a popcorn-like profile with blebs of basophilic material projecting from the surface or clusters of small, round, pyknotic bodies, which are characteristic of apoptosis. Such intrauterine inclusions were not seen in any tissues from negative controls. Interestingly, few lymphocytes were observed in most tissues from cases of hydrops fetalis caused by B19 infection.

Tissues were stained with TUNEL method (terminal deoxynucleotidyl transferase [TdT]-mediated deoxyuridine triphosphate-digoxigenin nick-end labeling) to examine apoptosis of individual cells. With the TUNEL immunostaining 3.5% to 14.0% of erythroid cells with characteristic inclusion bodies showed intense signals (Fig. 8C). The percentages of TUNEL positivity varied among cases. Less than 1% of erythroid cells in control tissues had positive signals. To confirm apoptosis of individual cells, tissues were double-stained with TUNEL and PAR3. All cells positive for TUNEL were also stained with PAR3, and the percentage of PAR3-positive cells that were also positive for TUNEL was 2.5% to

12.0%. In erythroid cells, the rate of double-staining was correlated with that of characteristic inclusions.

Propagation of B19 virus in primary culture of erythroid lineage cells derived from fetal liver

Hydrops fetalis is thought to be caused by infection of B19 to fetal erythroid lineage cells during pregnancy. We examined whether B19 virus infected erythroid lineage cells derived from fetal liver, in which erythropoiesis occurs actively.

Liver tissues were obtained from aborted fetuses ranging in gestational age from 18 to 21 weeks. This study was approved by the Ethic Committee of Tohoku University School of Medicine. Erythroid cells were enriched from the tissues, incubated with B19 virus, and cultured in RPMI 1640 medium supplemented with 20% fetal calf serum, interleukin 3 and erythropoietin. The expression of B19 virus antigen was examined by indirect immunofluorescence staining with the monoclonal antibody, PAR3.

On day 4 of postinfection, the intensity of fluorescence became maximal and the percentage of positive cells increased to 5% (Fig. 9). After day 8, the number of positive cells decreased gradually. To confirm the specific infection with B19 virus, we carried out an experiment to test the ability of human anti B19 virus-positive sera to neutralize B19 virus. In vitro infection of B19 virus in the cells was completely neutralized by the addition of anti-B19 virus positive sera but not by negative sera. Although erythroid lineage cells were enriched, it obviously contained other cell lineage population as well. We wished to identify the lineage of cells that were infected with B19 virus. The infected cells were stained doubly with human anti-B19 virus positive serum and mouse monoclonal antibody, EP-1, specific for burst-forming unit of erythroid and colony-forming unit of erythroid. Cells stained with anti-B19 virus positive serum were always stained with EP-1, and about 20% of EP-1 positive cells expressed B19 virus

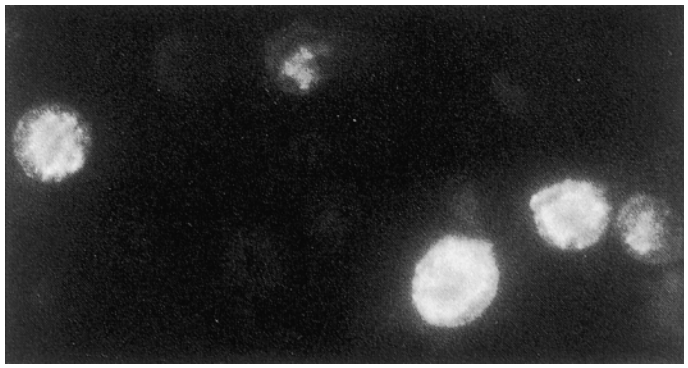

Fig. 9. Indirect immunofluorescence staining with PAR3 for cells harvested on day 2 after in vitro infection. Immunofluorescence staining of B19 virus-infected cells. Fetal erythroid lineage cells were infected with B19 virus. On day 4 of postinfection, the cells were stained by PAR3, anti-B19 monoclonal antibody.

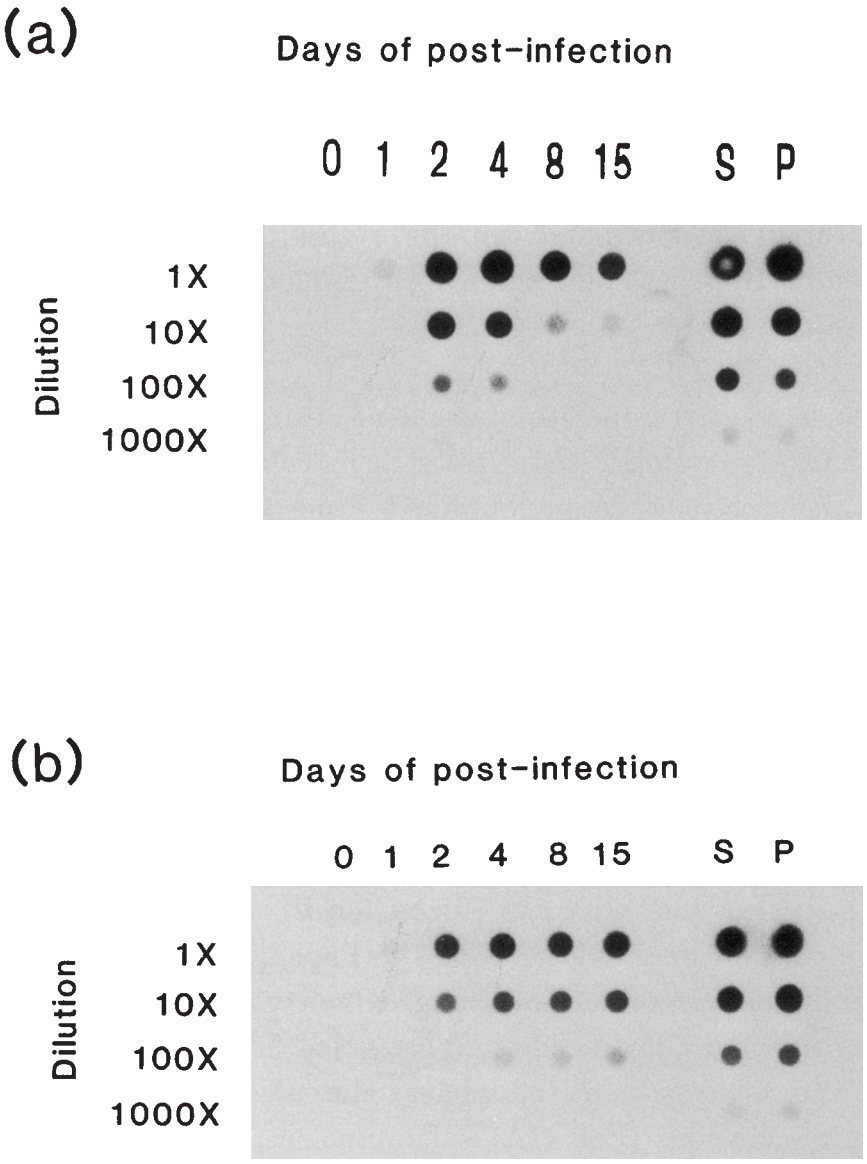

Fig. 10. Viral DNA production in the B19 virus-inoculated erythroid lineage cell culture. DNA was extracted from the cells (a) or culture supernatants (b) harvested. Their B19 virus DNA contents were determined by dor blot hybridization with a B19 virus DNA probe. DNA extracted from 1 μl of B19 virus antigen-positive serum (S) and 10 ng of DNA of teh probe (P) were used as controls. These DNA samples were serially diluted.

antigen. These results indicated that B19 virus could infect and propagate in erythroid lineage cells in human fetal liver (Yaegashi et al. 1989c).

Replication of B19 viral DNA in the erythroid lineage cells was examined by quantitatively determining the amount of viral DNA in the cells and culture supernatants. We used the dot blot hybridization method and estimated the concentration of viral DNA in samples (Fig. 10). B19 virus-specific DNA could be detected in the cells on day 1 of post-infection and maximally present in the sample from cells on day 2. Even a DNA sample from the day 15 showed the existence of the B19 virus genome in the cells. B19 virus-specific DNA was similarly detected in preparations from culture supernatants. The content of B19 virus gradually increased. These results indicated that the B19 virus genome

replicates in erythroid lineage cells from human fetal liver and that B19 virions are released from these infected cells.

We next addressed the question of whether the B19 virus generated in the in vitro system was infectious. B19 virus in the supernatant from the culture 15 days after infection was inoculated into the erythroid lineage cells from fetal liver. B19 virus-specific DNA was detected in cell extracts on day 4 of postinfection.

Apoptosis of cells infected in vitro

UT7/Epo is an erythropoietin-dependent strain of a megakaryoblastic cell line (Shimomura et al. 1992). In vitro B19 inoculation of cells was performed with B19 antigen-positive serum obtained from a patient with erythema infectiosum (the generous gift of Dr. H. Sato, Fukuoka) at 4°C for 2 hours. Cells were cultured in RPMI-1640 medium supplemented with 10% fetal calf serum and 2 units/ml of recombinant erythropoietin in a humidified incubator at 37°C with 3% CO_2. Control cultures were mock-infected with normal human serum. At periods between 1 and 4 days after infection, infected cells were harvested and analyzed with pathologic and biochemical methods.

On days 1 and 4 postinfection, approximately 25% of UT7/Epo cells infected in vitro were positive for B19 viral capsid protein by indirect immunofluorescence staining with PAR3 and all mock-infected cells were negative. Smears for cytologic examination were stained with the Papanicolaou method. Many cells showed a striking pattern of nuclear change which was distinct from that of mock infection. In infected cultures, ground-glass-like homogeneous eosinophilic nucleated cells were observed and the nuclear chromatin was spread as a thin rim around nuclear inclusions (Fig. 11A). The nucleus often showed small, round, pyknotic bodies characteristic of apoptosis (Fig. 11B). These characteristic cells

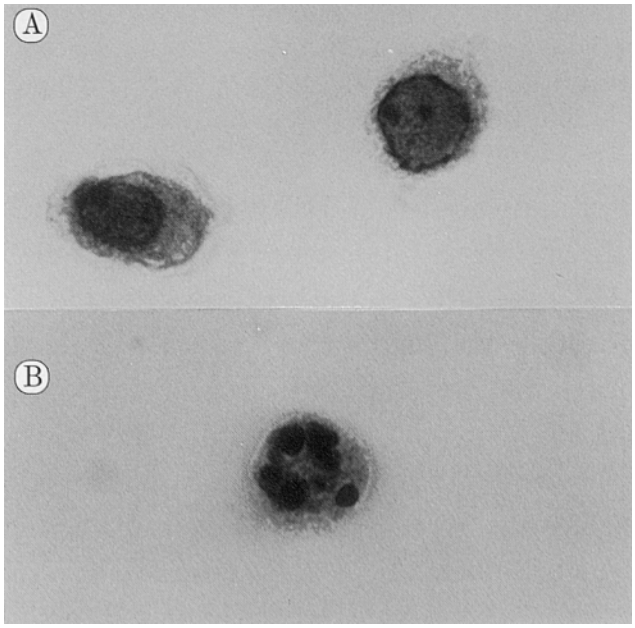

Fig. 11. Papanicolaou staining of cells harvested on day 4 after infection.

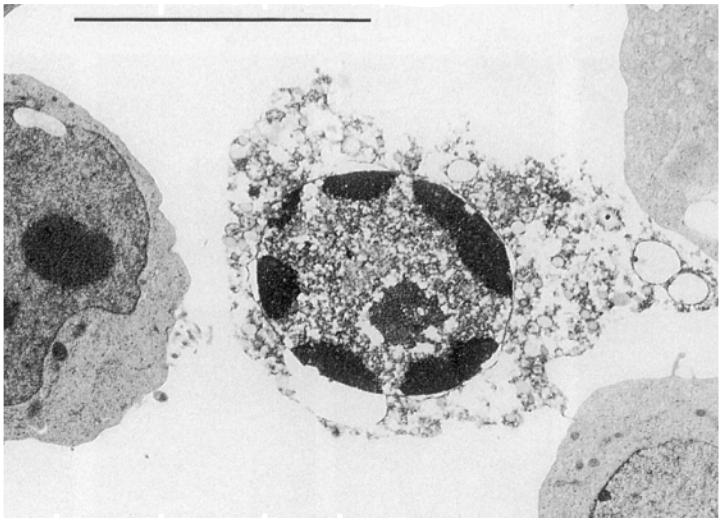

Fig. 12. Electron microscopic features and DNA fragmentation of UT7/Epo cells infected in vitro. On day 4, the nuclei showed several crescent-shaped clumped masses with increased density, and the cytoplasm of affected cells were filled with numerous vacuoles.

were not observed in mock-infected cultures. The cells were doubly stained with PAR3 and TUNEL to confirm apoptosis of individual cells. The percentage of TUNEL-positive cells among PAR3-positive cells increased with the length of culture: less than 1% on day 1, 23% on day 2, and 40% on day 4. TUNEL-positive cells were not observed in mock-infected cultures. DNA fragmentation analysis by gel electrophoresis showed the characteristic DNA fragmentation into a 180- to 200-bp ladder for cells infected in vitro. Mock-infected cells did not cause any demonstrable DNA laddering. These results indicate that B19 infection in vitro induces apoptosis of infected cells.

Cells infected in vitro were then examined electron microscopically. On day 2, cells contained clusters of electron-dense particles of approximately 20 nm in diameter in both the nucleus and the cytoplasm and showed peripherally condensed heterochromatin. On day 4, the nuclei of infected cells contained several crescent-shaped clumps of heterochromatin with increased density, the cytoplasm contained numerous vacuoles, and the cells themselves became smaller (Fig. 12). These changes are characteristic of apoptosis. No cells in mock-infected cultures showed such nuclear changes.

NS1 protein of B19 induces apoptosis in erythroid lineage cells

Infection of erythroid-lineage cells by B19 virus is characterized by a gradual cytocidal effect, which is related to apoptosis. Accumulating evidence now implicates the nonstructural protein (NS1) of the virus in cytotoxicity, but the mechanism underlying the NS1-induced cell death is not known. Using a stringent regulatory system, we demonstrated that the expression of the NS1 protein in erythroid lineage cell lines induces apoptosis of the cells (Moffatt et al. 1998).

K562 and UT7/epo, erythroid lineage cell lines, were used to examine the

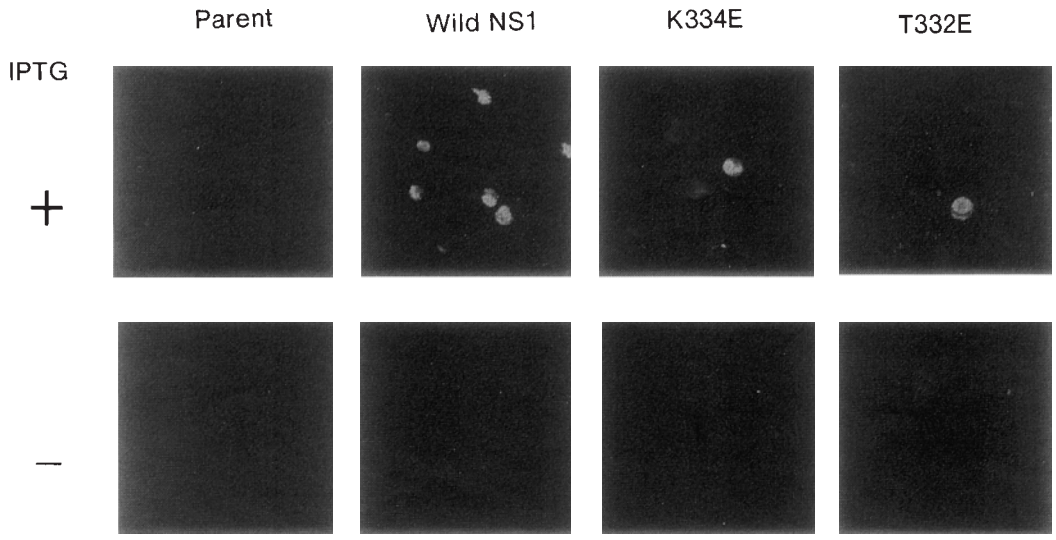

Fig. 13. TUNEL immunostaining in K562 cell lines with NS1 protein expression. TUNEL immunostaining shows the parents, K334E mutants, T332E mutant, and the wild-type NS1 cells with (uppeer palels) and without (lower panels) IPTG inductions.

cytotoxic activity of NS1. The *Escherichia coli* lac repressor-operator system was used to control NS1 expression. The expression of NS1 under the control of IPTG was observed only under inducing conditions. We observed that the initiation of cell death occurred after 24 hours of the induction of the NS1 protein. The death cells showed apoptotic appearance, with cell rounding, chromatin condensation, cytoplasmic blebbing, and characteristic DNA fragmentation into a 180- to 200-bp ladder as shown by gel electrophoresis. Using the TUNEL staining method, we detected cells positively stained for fragmented DNA (Fig. 13). These results suggest that NS1 mediates the apoptosis of these erythroid cell lines.

NS1 contains an NTP-binding motif in the middle of the protein, and the cytotoxicity mediated by NS1 is abolished by various mutations within the NTP-binding domain. We extended this line of study by asking whether disruption of this domain could ameliorate NS1-mediated apoptosis by designing two single-point mutations; K334E (lysine to glutamate at position 334) and T332E (threonine to glutamate at position 332) with the original NS1 expression vector as a template. The mutants with disruption in the NTP-binding domain dramatically suppressed the cytotoxic activity of NS1, whereas the wild-type NS1-carrying cell lines showed a continued increase in cytotoxicity.

Detection of cellular factors associated with the apoptotic pathway

Tissue sections were immunohistochemically analyzed with antibodies against cellular factors in the signaling pathway of apoptosis. Intense signals were observed with the antibody to caspase3/CPP32 in 3.0% to 12.0% of erythroid cells in tissues from cases of hydrops fetalis caused by B19 but not in control tissues. No positive signals were detected with antibodies to caspase1/ICE,

caspase2/ICH-1, FAS, Bcl-2, perforin, or granzyme B. Of the erythroid cells with inclusions, 2.5% to 6.0% had positive signals with antibodies against p53 and 1.5% to 5.5% against p21/WAF1. Erythroid cells in control tissues were not stained with any antibodies.

Comments

Intrauterine B19 infection often causes hydrops fetalis and fetal deaths. The pathgenesis of hydrops fetalis is based on the tropism of B19 virus for erythroid precursor cells in fetal liver. The NS1 protein encoded by the B19 genome induces apoptosis of erythroid lineage cells infected with B19, which is the main mechanism of fetal death. To analyze NS1 functions in vivo to induce fetal hydrops, we are trying to establish transgenic mice with the NS1 gene of B19.

Acknowledgments

This research was supported by a grant from the Ministry of Education, Science, Sports and Culture of Japan and by a grant from Nichibo Ogyaa Donation Foundation. This research was performed by great helps of many people and I specially thank Kohtaro Tada, Ryoko Mamiya, Hiroyuki Shiraishi, Takenari Niiuma, Hiroshi Chisaka, Stanley Moffatt, Professor Kunihiro Okamura, Professor Akira Yajima and Professor Kazuo Sugamura.

References

1) Brown, T., Anand, A., Ritchie, L.D., Clewley, J.P. & Reid, T.M.S. (1984) Intrauterine parvovirus infection associated with hydrops fetalis. *Lancet*, **2**, 1033-1034.
2) Brown, K.E. & Young, N.S. (1998) Human parvovirus B19 infections in infants and children. *Adv. Pediatr. Infect. Dis.*, **13**, 101-126.
3) Cossart, Y.E., Field, A.M., Cant, B. & Widdows, D. (1975) Parvovirus-like particles in human sera. *Lancet*, **1**, 72-73.
4) Knott, P.D., Welply, G.A.C. & Anderson, M.J. (1984) Serologically proved intrauterine infection with parvovirus. *Br. Med. J.*, **289**, 1660.
5) Moffatt, S., Yaegashi, N., Tada, K., Tanaka, N. & Sugamura, K. (1998) Human parvovirus B19 non-structural (NS1) protein induces apoprosis in erythroid lineage cells. *J. Virol.*, **72**, 3018-3028.
6) Sasaki, T., Takahashi, Y., Yoshinaga, K. & Sugamura, K. (1989) An association between human parvovirus B19 infection and autoantibody production. *J. Rhuem.*, **16**, 708-709
7) Sasaki, T., Murai, C., Muryoi, T., Takahashi, Y., Munakata, Y., Sugamura, K. & Abe, K. (1995) Persistent infection of human parvovirus B19 in a normal subject. *Lancet*, **341**, 851.
8) Shimomura, S., Komatsu, N., Frickhofen, N., Anderson, S., Kajigaya, S. & Young, N.S. (1992) First continuous propagation of B9 parvovirus in a cell line. *Blood*, **79**, 18-24.
9) Shiraishi, H., Wong, D., Purcell, R.H., Shirachi, R., Kumasaka, T. & Numazaki, Y. (1985) Antibody to human parvovirus in outbreak of erythema infectiosum in Japan. *Lancet*, **1**, 982-983.
10) Shiraishi, H., Umene, K., Yamamoto, H., Hatakeyama, Y., Yaegashi, N. & Sugamura, K. (1989) Human parvovirus (HPV/B19) infection with purpura. *Microbiol. Immunol.*, **33**, 369-372.
11) Shiraishi, H., Sasaki, T., Nakamura, M., Yaegashi, N. & Sugamura, K. (1991)

Laboratory infection with parvovirus B19. *J. Infect.*, **17**, 308-310.
12) Yaegashi, N., Shiraishi, H., Tada, K., Yajima, A. & Sugamura, K. (1989a) Enzyme-linked immunosorbent assay for IgG and IgM antibodies against human parvovirus B19: Use of monoclonal antibodies and viral antigen propagated in vitro. *J. Virol. Methods*, **26**, 171-182.
13) Yaegashi, N., Tada, K., Shiraishi, H., Ishii, T., Nagata, K. & Sugamura, K. (1989b) Characterization of monoclonal antibodies against human parvovirus B19. *Microbiol. Immunol.*, **33**, 561-567.
14) Yaegashi, N., Shiraishi, H., Takeshita, T., Nakamura, M., Yajima, A. & Sugamura, K. (1989c) Propagation of human parvovirus B19 in primary culture of erythroid lineage cells derived from fetal liver. *J. Virol.*, **63**, 2422-2426.
15) Yaegashi, N., Okamura, K., Hamazaki, Y., Yajima, A., Shiraishi, H. & Sugamura, K. (1990) Prevalence of anti-human parvovirus antibody in pregnant women. *Acta Obstet. Gynecol. Jpn.*, **42**, 162-166.
16) Yaegashi, N., Okamura, K., Yajima, A., Murai, C. & Sugamura, K. (1994) The frequency of human parvovirus B19 infection in nonimmune hydrops fetalis. *J. Perinat. Med.*, **22**, 159-163.
17) Yaegashi, N., Okamura, K., Tsunoda, A., Nakamura, M., Sugamura, K. & Yajima, A. (1995) A study by means of a new assay of the relationship between an outbreak of erythema infectiosum and non-immune hydrops fetalis caused by human parvovirus B19. *J. Infect.*, **31**, 195-200.
18) Yaegashi, N., Niinuma, T., Chisaka, H., Watanabe, T., Uehara, S., Okamura, K., Moffatt, S., Sugamura, K. & Yajima, A. (1998) The incidence of and factors leading to parvovirus B19-related hydrops fetalis following maternal infection; report of 10 cases and meta-analysis. *J. Infect.*, **37**, 28-35.
19) Yaegashi, N., Niinuma, T., Chisaka, H., Uehara, S., Okamura, K., Shinkawa, O., Tsunoda, A., Moffatt, S., Sugamura, K. & Yajima, A. (1999a) Serologic study of human parvovirus B19 infection in pregnancy in Japan. *J. Infect.*, **38**, 30-35.
20) Yaegashi, N., Niinuma, T., Chisaka, H., Uehara, S., Moffatt, S., Tada, K., Iwabuchi, M., Matsunaga, Y., Nakayama, M., Yutani, C., Osamura, Y., Okamura, K., Sugamura, K. & Yajima, A. (1999b) Parvovirus B19 infection induces apoptosis of erythroid cells in vitro and in vivo. *J. Infect.*, **39**, 68-76.